

Quantum state manipulation and cooling of ultracold molecules

Received: 18 May 2023

Accepted: 30 January 2024

Published online: 16 May 2024

 Check for updates

Tim Langen^{1,2}, Giacomo Valtolina³, Dajun Wang⁴ & Jun Ye⁵✉

In recent years, an increasingly large variety of molecular species have been successfully cooled to low energies, and innovative techniques continue to emerge to reach ever more precise control of molecular motion. In this Review, we focus on two widely employed cooling techniques that have brought molecular gases into the quantum regime: association of ultracold atoms into quantum gases of molecules and direct laser cooling of molecules. These advances have brought into reality the capability to prepare and manipulate both internal and external states of molecules on a quantum mechanical level, opening the field of cold molecules to a wide range of scientific explorations.

Over the past two decades, research on cold molecules has blossomed from a nascent field into a strong scientific current that expands the horizon of physical sciences^{1–3}. The scientific community is currently witnessing a transition from early aspirations to impactful scientific fruition and emergent technology. Pioneering ideas of cooling molecules to unexplored low-energy regimes^{4,5} have led the way to a more mature pursuit of goal-driven molecular quantum state control⁶. Chemical interactions are being studied with much greater details, including individual reaction pathways and resonances^{7–9}. Molecular complexity has become a feature to demonstrate sophisticated quantum control and explore emergent phenomena^{10–15}. Several ideas for the implementation of tunable many-body Hamiltonians with long-range, anisotropic interactions through the manipulation of molecules with external fields have expanded quantum simulation prospects^{16–20}. Molecules with extended coherence times are now setting more stringent limits and opening novel grounds for quantum sensing and for the exploration of fundamental symmetry and new physics beyond the standard model^{21–23}. Moreover, increasingly precise control of complex molecules fits right into the emergent theme of quantum information, which builds on high-fidelity manipulation of microscopic quantum systems^{24–27}.

Given the central role that molecules play in a wide range of physical processes, the progress in the field of cold molecules is bringing together scientists from many different disciplines. Particle physicists are interested in using molecules to search for evasive particles and fields. Condensed-matter physicists are building quantum material

models based on cold molecules. Chemists aim to improve the elementary understanding of the most fundamental reaction processes to enable designer chemistry. Quantum scientists are using molecules to build quantum simulation and information processing platforms. More complex molecules might also enable powerful technologies that are attractive to biomedical researchers²⁸.

Molecules bring us great diversity and a rich energy-level structure, and their control and use for scientific exploration thus demand a wide scope of methods and approaches. Although it is easy to judge the success of molecular cooling by the temperatures achieved, scientific vision and purpose should always be the foremost guiding principle when designing and deciding research directions on cold molecules.

In this Review, we present a selected few approaches that are being effectively pursued for the cooling, trapping and manipulation of molecules, and a few examples of scientific successes that build upon these tools. These efforts underpin our goal of precise control of molecular states for achieving a comprehensive understanding of emergent complexity in quantum materials, controlled chemical processes, and powerful new methods for precision measurement and quantum information science. The purpose of this Review is to provide a common connection between varying approaches to cold molecules and their relevant scientific goals.

Preparation of ultracold molecules

In this first section, we discuss recent progress in the cooling and trapping of molecules. We focus on two distinct methods, namely,

¹Physikalisches Institut and Center for Integrated Quantum Science and Technology (IQST), Universität Stuttgart, Stuttgart, Germany. ²Vienna Center for Quantum Science and Technology, Atominstitut, TU Wien, Vienna, Austria. ³Fritz-Haber-Institut der Max-Planck-Gesellschaft, Berlin, Germany.

⁴Department of Physics, The Chinese University of Hong Kong, Hong Kong SAR, China. ⁵JILA and Department of Physics, National Institute of Standards and Technology and University of Colorado, Boulder, CO, USA. ✉e-mail: ye@jila.colorado.edu

the association of quantum gases of atoms into ultracold molecules and direct laser cooling of molecules. These approaches are leading the production of molecular samples with high phase-space densities and full control over quantum mechanical degrees of freedom.

We note that there exists a further large variety of powerful techniques and strategies to control the external and internal degrees of freedom of molecules, which we mention here only briefly. These include buffer gas²⁹ and supersonic sources^{30,31}, decelerators³² and their combination with conservative traps^{33,34}, merged³⁵ or crossed³⁶ molecular beams, as well as cryofuges³⁷ and Sisyphus cooling of electrically trapped molecules³⁸. We also note that there is a whole vibrant field of trapped molecular ions that have been used for studies of chemical reaction dynamics, precision measurement and quantum logic gates³⁹.

Association of quantum gases of atoms

The first strategy that we discuss here in detail relies on the ability to create and manipulate gases of ultracold atoms^{40,41}. By ramping an external magnetic field across a Feshbach resonance, pairs of these atoms can be associated into weakly bound, highly excited Feshbach molecules⁴² (Fig. 1a). Transfer of these molecules into their absolute ground state can be realized by stimulated Raman adiabatic passage (STIRAP). In this process, a pair of Raman lasers coherently transfers the molecules into their ground state via a suitable excited state. This removes thousands of kelvins worth of binding energy from a gas at nanokelvin temperatures. The coherence of the process is essential for this, as any spontaneous processes would unavoidably lead to undesirable heating.

A key ingredient is the choice of the excited state that must accommodate the vastly different vibrational wavefunction extension as well as the different—typically singlet and triplet—characters between the Feshbach molecule and the ground-state molecule, respectively, to provide sufficient transition strengths for both legs of the Raman transfer. Although such a state can in general be found through extensive spectroscopy with the help of detailed knowledge on the molecular structure, the Rabi frequencies, especially that for the upwards transition, are often not very high. In this limit, high STIRAP efficiency can be achieved with only long-duration Raman pulses, which require high relative phase coherence between the Raman lasers. In earlier work, this was established by phase locking the Raman lasers to a stabilized frequency comb^{43,44}. Currently, the comb has been replaced by high-finesse ultrastable cavities with dual-wavelength coating⁴⁵. With these efforts, a one-way STIRAP transfer efficiency of over 90% has been achieved. The high efficiency is also important for detection, which relies on the reversed STIRAP process to transfer ground-state molecules back to the Feshbach state.

Association of ultracold atoms has so far achieved the highest phase-space densities in molecular gases. However, as this strategy requires ultracold atomic gases to start with, it produces only molecular species formed from atomic species that can be laser cooled. Typical experimental examples are heteronuclear^{43,46–53} and homonuclear⁵⁴ mixtures of alkalis, or mixtures of alkali and alkaline earth atoms⁵⁵.

A related technique to magneto-association is photo-association of ultracold atoms, which has also been used to create bi-alkali molecules in the rovibrational ground state^{45,56,57}. Further work has also suggested the possibility to form alkali–lanthanide and alkaline earth–lanthanide mixtures with large spins^{58,59}.

Notably, recent progress has led to the first generation of quantum degenerate molecular Fermi gases of KRb (Fig. 1b) and NaK molecules^{60–64}, as well as the first Bose–Einstein condensate (BEC) of NaCs molecules⁶⁵. Moreover, the technique not only works for mesoscopic gases of many particles but also can be applied even on the single-molecule level, where precisely two atoms can be turned into one molecule^{66–68}.

The molecular quantum gases created in this approach are readily loaded into optical dipole traps or optical lattices, leading to studies

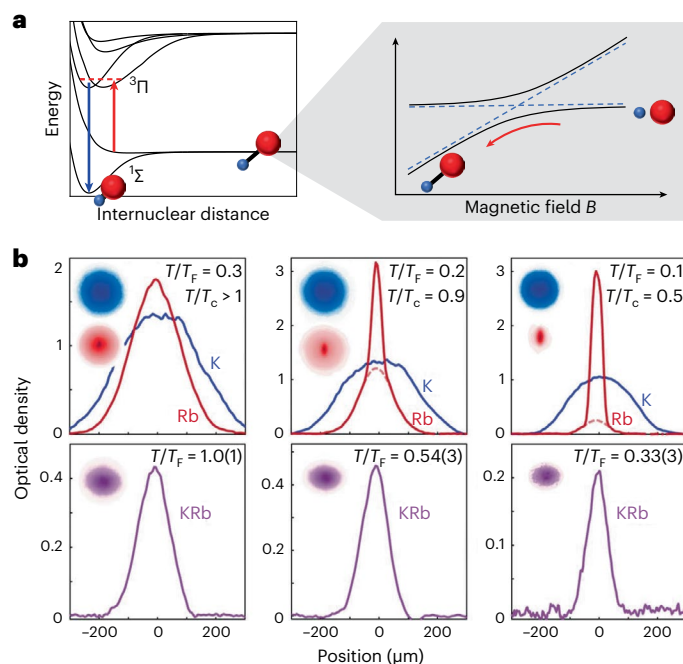


Fig. 1 | Preparation of ultracold molecules from ultracold atoms. a, Magneto-association and STIRAP transfer. Pairs of atoms are associated into a weakly bound molecule by sweeping a magnetic field over a scattering resonance (inset). These weakly bound molecules are subsequently transferred into the rovibrational ground state by a two-colour STIRAP via an excited state. **b**, Transition of a mixture of potassium and rubidium clouds (top) and associated KRb molecules from these clouds (bottom) into the quantum degenerate regime. Temperatures T decrease from left to right, with T_c being the critical temperature for the bosonic Rb atoms and T_F representing the individual Fermi temperatures for the fermionic K atoms and KRb molecules, respectively. Panel b adapted with permission from ref. 60, AAAS.

of chemical reactions near absolute zero^{15,69}, long lifetimes of trapped molecules^{70,71}, tuning of state-dependent trapping potentials^{72,73} and spin-exchange interactions^{16,17,19,26,74}.

Direct laser cooling

Laser cooling relies on the repeated scattering of photons. Through this photon cycling, the collective actions of tens of thousands of photons, each with a small individual momentum, lead to sizable forces for massive particles such as atoms or molecules. Thus molecules, with their complex internal structure, do not, a priori, appear to be very well suited for laser cooling, as an excitation created by absorbing a photon can easily decay into many vibrational and rotational energy levels different from the initial one. As each of the corresponding transitions has a different frequency, photon cycling appears to require an unpractically large number of lasers to address all of these transitions.

However, over the past decade, it has been established that this challenge can be overcome in a large number of molecular species, by exploiting diagonal Franck–Condon factors⁴ and transition selection rules⁵ to limit vibrational and rotational branching. A study⁵ further proposed practical schemes for constructing a molecular magneto-optical trap. While these requirements again limit cooling to a subset of molecular species, the required properties are fairly generic and provide a large variety of chemically diverse species^{75–77}.

The best understood examples showing favourable vibrational properties are alkaline earth monofluorides (SrF (ref. 78), CaF (refs. 79, 80)) and oxides such as YO (refs. 81,82). The calculated valence electron distribution of the CaF ground state is shown in Fig. 2a. While one of the calcium atom's two valence electrons forms the molecular bond with the electronegative fluorine atom, the other one is primarily located

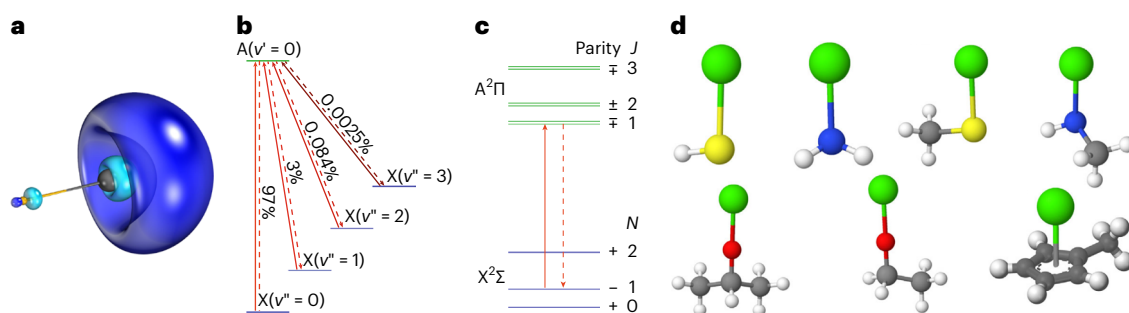


Fig. 2 | Laser cooling of molecules. **a**, The calculated valence electron distribution for the ground state of CaF molecules, where the optically active electron is centred around the metal atom and polarized away from the molecular bond. The molecule thus behaves similarly to an alkali atom, with transitions of the single valence electron independent from molecular vibrations to a very good approximation. **b**, This leads to a highly diagonal Franck–Condon factor (between the lowest vibrational levels $v'' = 0$ and $v' = 0$ of the electronic ground state X and the first excited state A), which strongly suppresses vibrational branching and limits the number of lasers required to realize a closed cooling cycle. **c**, In addition, rotational branching can be suppressed using parity

around the calcium atom and polarized away from the bond⁸³. Excitations of this latter electron are thus nearly unaffected by changes in the molecular vibrational state, leading to diagonal Franck–Condon factors and strongly suppressed vibrational branching (Fig. 2b). The molecules thus behave—in some ways—similarly to alkali atoms, which are common in atomic laser-cooling experiments. In YO, the same principle holds⁵ for two independent electron–nuclear spin angular momentum ground states, enabling efficient formation of a magneto-optical trap (MOT) and grey molasses sub-Doppler cooling⁸⁴. YO also features a narrow transition that can facilitate narrow line cooling similar to that in alkaline earth atoms⁸⁵.

Given the abundance of potential candidates, the list of explored molecular species is expected to grow rapidly in the coming years. In particular, favourable vibrational properties are not limited to diatomic species, but extend naturally to polyatomic ones, where a large variety of ligands can be attached to atoms or diatomics acting as optical cycling centres^{86,87} (Fig. 2d). Initially demonstrated with linear triatomic molecules such as SrOH, CaOH and YbOH (refs. 88,89), this approach has now also been extended experimentally to more complex molecules such as CaOCH₃ (ref. 12). The limits of this approach are currently very actively explored on the theoretical chemistry side, with the goal of systematically predicting which ligands are compatible with which cycling centres^{87,90,91}.

On the practical side, the additional structure of polyatomics leads to additional vibrational bending, stretching and hybrid modes, which require additional lasers to address the corresponding states. Although this increases the complexity of maintaining a nearly closed optical cycle, the overall structure of polyatomics is particularly favourable for precision measurements^{92–94} as it leads, for example, to opposite parity, nearly degenerate doublets of states. Such molecules can thus generically be polarized in electric fields that are much smaller than the fields required for diatomic molecules and their structure provides a powerful tool to control systematic effects in precision measurements. Other applications of polyatomic molecules that have been considered include quantum simulation, quantum computation, and ultracold chemistry and collisions⁸⁷.

For both diatomics and polyatomics, once vibrational branching is suppressed, angular momentum and parity selection rules for rotational states can be used in combination with remixing of dark states that are not addressed by the laser light, to realize a closed optical cycle^{5,82} (Fig. 2c). Recently, the work on species with more complex hyperfine structure, which show many additional dark states, has also gained traction^{95,96}.

selection rules, by driving transitions from the energetically lowest ground state with negative parity ($N = 1$) to the lowest excited state with positive parity ($J = 1, +$). **d**, A similar strategy can be followed to laser cool also more complex polyatomic molecules that are formed from a suitable optically active cycling centre (that is, an atom or diatomic molecule, shown here in colour) and a ligand (shown in greyscale). This ligand can, in principle, have very different levels of complexity without significantly perturbing the laser-cooling cycle. Panels adapted with permission from: **a**, ref. 166; **b,c**, ref. 75, Taylor & Francis; **d**, ref. 93, under a Creative Commons licence CC BY 4.0.

Turning a closed optical cycle into actual laser cooling requires the understanding of the resulting multi-level systems^{95,97,98}. Scattering rates in such multi-level systems are proportional to $N_e/(N_g + N_e)$, where N_e and N_g are the number of excited and ground states that are coherently involved in the optical cycle. Typical monofluorides, for example, show 4 excited and 12 ground states in each addressed vibrational level. The scattering rates are thus significantly reduced compared with the textbook two-level situation, which also goes hand in hand with increased saturation intensities for the transitions. Cooling of molecules therefore typically requires not only more lasers than cooling of atoms to address all required states but also higher laser powers to achieve sufficiently fast scattering.

However, apart from an increased level of complexity, one finds cooling forces similar to the ones known from atomic laser cooling, such as Doppler and Sisyphus forces. Molasses techniques can be used to image molecules down to the level of individual molecules⁹⁹. Interestingly, and in contrast to atoms, closed optical cycles can also be realized in ways where absorption and emission occur on different wavelengths, which allows near-background-free detection of molecules, for example, for precision measurement applications^{100,101}.

Experiments typically start with a slow molecular beam, formed, for example, by laser ablation and buffer gas cooling^{29,102}, which is laser slowed^{82,103,104} to the capture velocity of a magneto-optical trap^{78,80,89,105,106}. Further molasses cooling^{79,84,89} then produces molecular samples that can be trapped in conservative potentials^{107–111}.

The phase-space densities that have been achieved in this way have increased by more than 10 orders of magnitude in recent years, reaching now 10^{-6} (refs. 110,112), which is close to being suitable for further collisional cooling of the molecules to quantum degeneracy. Further progress is expected in the near future through more efficient slowing methods^{113–116}, more efficient sources¹¹⁷ and sympathetic cooling with atoms^{118,119}. The current phase-space densities are also sufficiently high to load optical tweezer arrays with single molecules¹²⁰, enabling studies of collisions on the single-molecule level¹²¹.

State engineering and coherence of single molecules

The rich internal structures of ultracold polar molecules, including their vibrational, rotational and hyperfine states, have long been identified as great assets for many potential applications. A prerequisite for exploring such possibilities is the capability of controlling the internal states of the sample on the single quantum level. Building on the

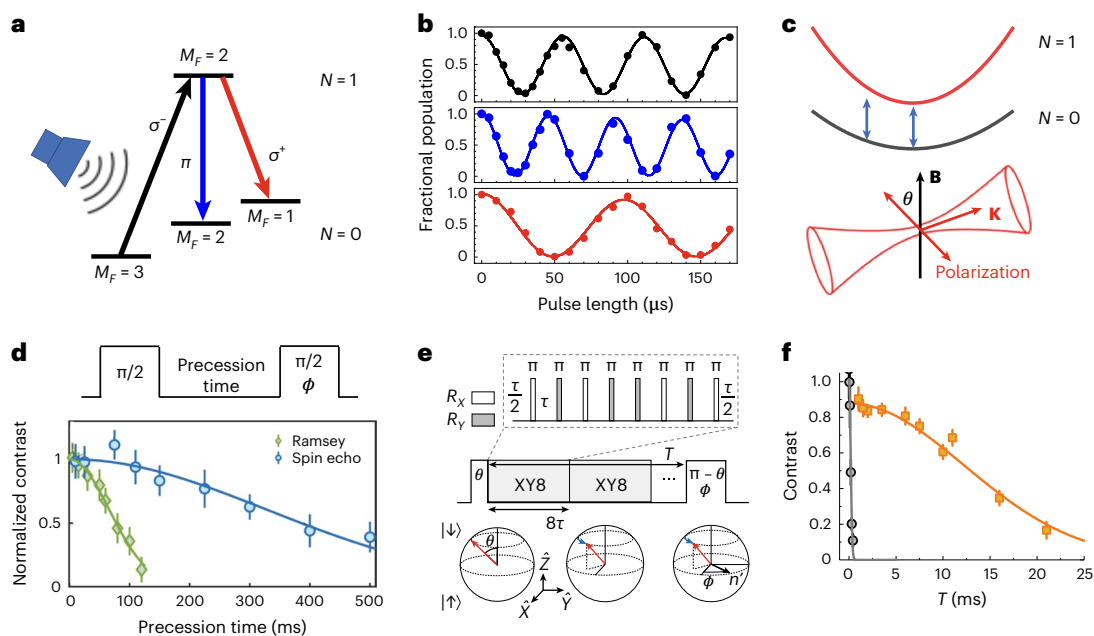


Fig. 3 | Internal state control and single-molecule rotational coherence.

a, Schematic of the microwave-driven transitions between rotational and hyperfine levels of NaRb. Here the projection of the total angular momentum $M_F = m_N + m_i^{\text{Na}} + m_i^{\text{Rb}}$ is always a good quantum number, with m_N , m_i^{Na} and m_i^{Rb} the projections of the rotation and atomic nuclear spins. A nuclear spin flip is made possible by nuclear spin and rotation mixing. **b**, Coherent population transfers from $N=0$ to $N=1$ or between hyperfine levels in $N=0$. The oscillations and their corresponding transitions in **a** are colour-coded. **c**, Differential light shifts cause rotational decoherence (top). This can be mitigated by tuning the polarization angle θ of the trapping light to the magic angle (bottom). The \mathbf{K} vector of the trapping light is perpendicular to the external magnetic field \mathbf{B} .

d, The rotational coherence time for single CaF molecules in optical tweezers is limited by a residual differential light shift (green diamonds). With spin echo, the coherence time is extended to nearly 500 ms (blue circles). Φ is the phase shift in the second $\pi/2$ Rabi pulse in the Ramsey spectroscopy for measuring the fringe contrast. **e,f**, Dynamical decoupling with the XY8 microwave pulse sequences which are implemented by adding eight Rabi π -pulses (R_x and R_y) spaced by time τ during the Ramsey evolution time T . (e) is powerful enough to extend the rotational coherence time of KRb molecules in 2D potentials to nearly 20 ms without the magic-angle compensation (f). Panels adapted with permission from: **a,b**, ref. 123, American Physical Society; **c,d**, ref. 131, APS; **e,f**, ref. 18 Springer Nature Ltd.

progress in cooling discussed in the previous section, this has been fully achieved with the combined power of optical and microwave methods. In addition, microwave coupling between rotational levels has emerged as a major method for engineering and probing intermolecular interactions. To fully explore the potential of this method, significant efforts have been devoted to understanding and controlling rotational coherence.

Internal state control

In magneto-association, the weakly bound Feshbach molecule is produced with a Feshbach resonance between atom pairs in single hyperfine Zeeman levels and is thus inherently in a single quantum level⁴². For bialkali molecules, the ground electronic state is $1^1\Sigma^+$, which has no electronic orbital and spin angular momenta. Their hyperfine structures are thus purely from the atomic nuclear spins and rotation¹²². In magnetic fields, these structures split into $(2N+1)(2I_1+1)(2I_2+1)$ closely spaced levels, with N the rotational quantum number, and I_i the nuclear spin of the two atoms. Take $^{23}\text{Na}^{87}\text{Rb}$ as an example: with $I_{\text{Na}} = I_{\text{Rb}} = 3/2$, there are 16, 48 and 80 levels for $N=0, 1$ and 2, respectively¹²³. In a magnetic field, the total frequency span of the hyperfine levels in each rotational state is on the megahertz level, while the intervals between adjacent hyperfine levels are even smaller. With the combination of selection rules and polarization, Rabi frequencies and the Raman laser pulse lengths, population transfer to single selected hyperfine levels has been routinely realized^{43,46–52}. However, it is worth mentioning that high spectroscopic resolution and high population transfer efficiency have contradictory requirements on Rabi frequencies. This highlights again the importance of establishing good phase coherence between the Raman lasers, which will allow high STIRAP efficiencies at lower Rabi frequencies and longer

pulses. If possible, using Feshbach resonances at higher magnetic fields to make hyperfine splitting larger also helps.

While most experiments start from molecules in the lowest energy level with vibrational and rotational quantum numbers $\nu=0$ and $N=0$, STIRAP can also place the population in $N=2$ directly. The $N=1$ level, which cannot be reached by STIRAP as limited by parity selection rules, can be populated with a microwave driving the rotational transition, for example, between $N=0$ and 1, as illustrated in Fig. 3a,b refs. 123–126. In addition, two-photon microwave transitions are also frequently used for hyperfine manipulation. As has been demonstrated in RbCs, multiple microwave frequencies can also be applied to produce molecules in higher rotational levels¹²⁷. STIRAP can also transfer molecules to low-lying excited vibrational states, such as $\nu=1$ (ref. 123). For molecules with no two-body chemical reactivity in the $\nu=0$ level, this can serve as a knob to turn on the reaction¹²⁸.

For directly laser-cooled $2^3\Sigma^+$ molecules, after the laser cooling stage the population is distributed in $N=1$, the state used for the realization of the closed laser-cooling cycle (Fig. 2c). This manifold contains multiple spin-rotation and hyperfine levels. In recent experiments with CaF and SrF molecules, preparing the molecules into a single hyperfine Zeeman level has been demonstrated using optical pumping and microwave driving^{107,109}. In combination with optical tweezers, such state control has facilitated the study of state-dependent collisions¹²¹, and entanglement of pairs of molecules via spin-exchange interactions^{26,27}.

Single-molecule coherence

The microwave coupling between rotational levels with opposite parities can induce strong dipolar interactions between molecules. This leads to a rotational dipolar spin-exchange interaction, which can be used for realizing a variety of spin models^{129,130} and implementing the

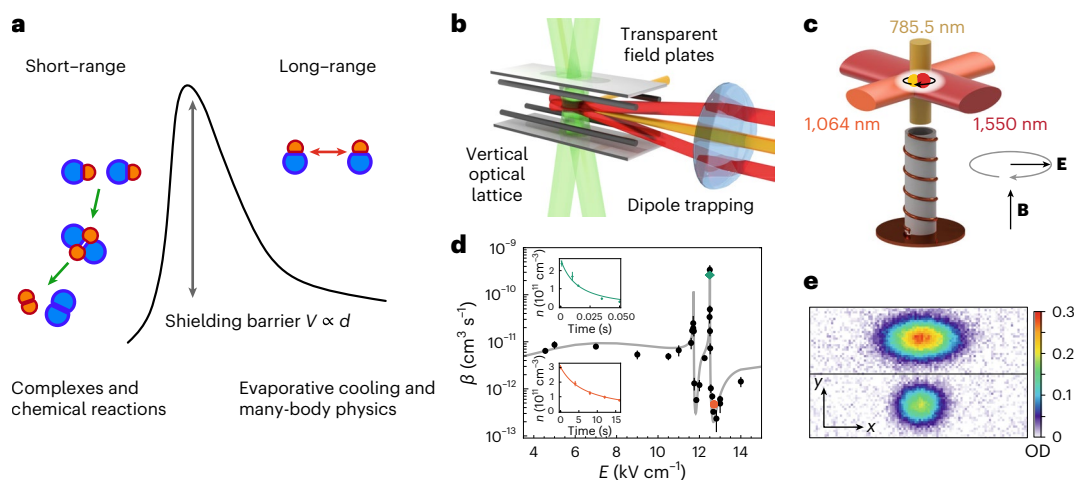


Fig. 4 | Controlling molecular interactions. **a**, Short-range versus long-range physics. The short-range regime happens inside the shielding barrier, whose height V is proportional to the induced dipole moment d , that can be controlled via external fields. The long-range regime is instead outside the barrier. At short-range, molecular collisions are dominated by complex formation and chemical reactions, and often result in losses. Dipolar interactions enable elastic scattering beyond the barrier, which is crucial for evaporative cooling and many-body physics. **b**, Experimental set-up for collisional shielding in 2D gases of ultracold molecules. 2D trapping is realized by a combination of dipole traps, and a well-controlled d.c. electric field is applied by transparent bias field plates

and auxiliary gradient rods. **c**, Experimental set-up for microwave shielding of ultracold molecules. Circularly polarized microwave electric fields are applied to molecules trapped in a combination of different dipole traps. **d**, Shielding resonance for KRB molecules in the $N = 1$ state as a function of the bias d.c. electric field E . The rate of two-body loss β is extracted from the evolution of the molecular density n at different values of E . The insets highlight the dramatic increase in molecular lifetime on different sides of the shielding resonance. **e**, Evaporative cooling of a 2D thermal Fermi gas of KRB molecules (top) to the quantum degenerate regime (bottom). Panels adapted with permission from: **b, e**, ref. 61, Springer Nature Ltd; **c**, ref. 62, Springer Nature Ltd; **d**, ref. 158, Springer Nature Ltd.

iSWAP two-qubit quantum gate^{24,25}. However, to make these applications possible, the single-molecule rotational coherence time must be longer than the timescale of the interaction.

For optically trapped molecules, the most important source of decoherence is the differential a.c. Stark shift^{72,73}, which causes shifts of the rotational transition frequencies across the trap. This problem can be mitigated using the anisotropic polarizability of $N = 1$. By setting the polarization of the trapping light to a ‘magic’ angle, as depicted in Fig. 3c, the light shifts of $N = 0$ and $N = 1$ from the scalar polarizabilities can be made exactly the same. However, the polarizability of $N = 1$ also has a tensor term that mixes the different rotational Zeeman levels m_N and results in a hyperpolarizability and a quadratic shift. This complication leads to an intensity-dependent magic angle, and more importantly an incomplete differential light-shift cancellation. The typical rotational coherence time, as measured by Ramsey spectroscopy, is limited to several milliseconds for bulk samples in optical traps⁷³. For single molecules in optical tweezers (Fig. 3d), a coherence time of 93(7) ms has been observed¹³¹.

Several different methods have been developed to make further improvements. Together with polarization-angle adjustment, a moderate d.c. electric field can be applied to decouple nuclear spins from rotation to minimize the hyperpolarizability and thus the intensity-dependent differential shift^{132,133}. Similarly, magnetic fields can be used to adjust the nuclear spin-rotation mixing to cancel the differential light shift at matched light intensities¹³³. For NaRb in the ground band of the two-dimensional (2D) optical lattices of a quantum microscope set-up, a coherence time of 56(2) ms has recently been reported¹⁹. A very different scheme is to create a ‘magic’ trapping potential for the different rotational states by tuning the trapping light to near resonance with an excited molecular state. To minimize off-resonance scattering, the nominally forbidden $\nu = 0 \leftrightarrow \nu = 0$ transition between $X^1\Sigma^+$ and $b^3\Pi$ is used^{134,135}. In RbCs, it is estimated that rotational coherence times greater than 1 s can be achieved in the magic potential¹³⁶.

Imperfections of the magnetic field, such as fluctuations and gradients, are another important source of decoherence. For $^1\Sigma^+$ molecules,

as the nuclear spins are very insensitive to magnetic fields, this is less of a problem. For $^2\Sigma^+$ molecules with a non-zero electron spin, the requirements on the magnetic field are in general more stringent. However, the sensitivity to magnetic field can be reduced significantly by choosing a pair of rotational hyperfine Zeeman levels with small relative shifts so that the rotational transition frequency has only a quadratic Zeeman shift at low magnetic fields^{26,27}.

To extend the rotational coherence time further, more advanced microwave pulse sequences, such as spin echo and dynamical decoupling, can be used to remove decoherence from quasi-static sources. In several experiments, coherence times of hundred of milliseconds were achieved with these methods in both optical lattices^{16,19} and optical tweezers^{26,27,131}. This is already much longer than the timescale of the dipolar interaction between molecules. Although more complex, dynamical decoupling pulse sequences are more powerful than spin echo^{26,27}. In the latest KRB experiment¹⁸, a coherence time of ~20 ms was achieved with an XY8 pulse sequence, despite the presence of large differential light shift between rotational states in an optical trap without using magic wavelength or magic angle (Fig. 3e,f).

Besides their insensitivity to magnetic fields, the nuclear spin hyperfine levels in $N = 0$ of $^1\Sigma^+$ molecules also experience very small differential light shifts⁷¹. They can thus serve as storage qubits for preserving quantum coherence over long periods of time^{24,25,137}. In several experiments, nuclear spin coherence times of several seconds have been observed in optical traps and lattices with two-photon microwave spectroscopy^{71,138,139}. Although it has not been demonstrated, with spin echo or dynamical decoupling, the nuclear spin coherence time should be readily extended to over 1 minute.

Molecular interactions

The exquisite control of interactions in atoms has enabled collisional cooling of laser-cooled atomic gases further into the ultracold regime, where collective quantum behaviour plays a leading role. Such a gas of indistinguishable particles with finely tunable interactions performs as a quantum simulator, providing insights in the behaviour of complex many-body systems. However, the class of phenomena that ultracold

atoms can explore is restricted by the limited strength, range and isotropic nature of their interactions.

Richer dipolar interactions with anisotropic and long-range character can be realized in magnetic quantum gases. This has recently led to the surprising observation of new states of matter such as droplets and supersolids^{140,141}. Nonetheless, the strength of this interaction is still inherently set and limited by the atomic structure. An ultracold and dense gas of polar molecules, with strong electric long-range interactions and a rich structure of coherent, long-lived states, is expected to greatly exceed the possibilities of such weakly dipolar atoms and realize new phases of matter, such as topological superfluids^{2,142}.

However, the very same complexity that makes molecules so appealing renders the precise control of their interactions highly challenging. Molecular collisions at short distance are not as favourable as atomic ones: their dense spectrum of internal energy levels allows two colliding molecules to stick together^{143,144} and undergo a (photo-) chemical reaction that hampers collisional cooling and most molecular quantum applications (Fig. 4a). Over the past decade, there has been tremendous efforts in understanding the collisional complexes that molecules form at short range, how they impact chemical reactions and how we can suppress their formation with shielding methods^{145–148}. Shielding has enabled the achievement of a new regime, a molecular gas dominated by elastic interactions, which can then be cooled to quantum degeneracy to study complex dipolar systems.

Ultracold chemical reactions and shielding methods

At ultralow temperatures, chemical reactions do not follow an Arrhenius-type equation as thermal energy is too low to overcome reaction barriers. Instead, wavefunction overlap and quantum tunnelling provide a way for molecules to meet at short distance and then react. Fermionic KRb ground-state molecules proved to be a valuable test bed for such ultracold chemistry. The reaction $\text{KRb} + \text{KRb} \rightarrow \text{K}_2 + \text{Rb}_2$ is energetically allowed and proceeds according to a two-body loss rate. By changing the initial state of the molecular gas, it is possible to tune the reaction rate in a quantum state-resolved fashion. Owing to the centrifugal barrier in the p-wave channel, a gas of identical fermionic molecules reacts less than a gas of distinguishable (or bosonic) molecules⁶⁹, where collisions in the barrier-less s-wave channel are allowed. Thus, control over the long-range barrier translates into control over the reactivity and stability of the molecules. This is the basic principle of reaction shielding. As anisotropic dipolar interactions mix higher-order partial waves together, they provide a way to change the height and shape of the long-range barrier.

Dipolar interactions can be induced by polarizing molecules in an external electric field. Initially, collisions of molecules in the lowest rotational level were investigated in a static electric field. While perpendicularly to the electric field dipolar interactions are repulsive, they are attractive along the field direction and facilitate short-range collisions. For a three-dimensional (3D) gas, the attractive dipolar component dominates and the rate of chemical reactions monotonically increases with the induced dipole moment¹⁴⁹. In 2D traps, it is possible to retain only the repulsive side of dipolar interactions when the 2D gas is tightly confined along the field direction (Fig. 4b). This shielding method combines strong dipolar interactions with optical lattice confinement to exploit the stereodynamics of the reaction and suppress the reaction rate with respect to the 3D case¹⁵⁰.

The technical complication in dealing with the large electric fields required for this type of shielding shifted the focus towards the creation of inherently chemically stable ultracold molecular samples^{46–49,51}. Surprisingly, the new species investigated for this purpose still showed two-body losses close to the universal limit of chemically reactive molecules^{128,151,152}. In 2019, a theoretical study¹⁴⁴ analysed the effect of optical dipole traps on molecular collisions, focusing on the role of intermediate complexes. Complexes are formed when molecules meet at short range. For chemically stable molecules, energy conservation should

allow complexes to dissociate back to the original reactants, while in the reactive case, complexes can transform into reaction products. In the alkali case, complexes have a broad optical absorption spectrum that peaks in the wavelength range of standard optical dipole traps. As a result, alkali complexes quickly absorb trap photons, heat up and are quickly lost from the trap. The detrimental role of optical trapping was later confirmed by two separate experiments^{153,154}. However, the features of complexes are far from being completely understood, as additional experiments with different molecular species observed persisting losses even in absence of optical traps^{155,156}.

Methods that shield molecular collisions from losses at short range completely are thus expected to become an integral part of molecular quantum gases experiments.

On the basis of the idea originally proposed in ref. 145, the first resonant shielding was achieved experimentally using molecules in large static electric fields, exploiting the rotational structure of polar molecules^{157,158} (Fig. 4d). In such a situation, resonant dipolar coupling results in a huge modulation of the chemical reaction rate in a narrow electric-field region around the energy-level crossing of pairs of rotational states coupled by the dipolar interactions. The shielding resonance enabled the realization of long-lived molecular gas in a static electric field.

Similarly, based on other theoretical ideas^{147,148}, ref. 159 exploited microwave radiation to engineer an effective repulsion between two-body collisions of CaF molecules in optical tweezers. Through proper detuning of the circularly polarized microwaves, it was possible to suppress reaction rates by a factor of six even in tight tweezer traps.

Dressing with strong microwave fields not only allows for shielding of collisions but also shows great promise to independently control elastic interactions at short range altogether. By finely tuning the ellipticity of the microwave, it is possible to bring the open channel of two colliding molecules into resonance with a weakly bound tetramer state^{148,160}. Control over the so-called field-linked resonance has enabled strong modulation of chemical reaction rates, but in the future it may be possible to coherently populate the tetramer state, similarly to the case of Feshbach molecules on a Feshbach resonance¹⁶¹. Full control over resonant dipolar scattering and short-range interactions, for example, by combining microwave shielding with additional d.c. electric fields, will enable the realization of the molecular analogue of the BEC–Bardeen–Cooper–Schrieffer (BCS) crossover and the attainment and stabilization of molecular BECs¹⁴².

Resonances in molecular collisions can also be controlled with external magnetic fields. Similarly to ultracold atoms close to a Feshbach resonance, atom–molecule¹⁶² and molecule–molecule¹³ collisions can show resonant behaviour, which results in a sharp increase of the loss rate of the trapped molecular gas. These resonances emerge when a long-range polyatomic (tri- or four-body) bound state can be brought to degeneracy with the scattering continuum. Precise control over their relative position enables new possibilities for coherent chemistry and molecule assembly. For instance, in collisions between sodium atoms and sodium–lithium molecules, an atom–molecule Feshbach resonance enabled the manipulation of the long-range barrier via control of the phase of the scattering wavefunction¹⁶³. Interference between the long-range and the short-range part of the molecular potential resulted in a strong modulation of the reaction rate, even exceeding the universal limit.

Evaporative cooling and quantum degeneracy

Shielding presents a twofold advantage: while short-range losses are quenched from the effective shielding repulsion, elastic collisions at long range are increased. Thus, shielding enables the realization of stable and strongly dipolar molecular gases, with large ratios of elastic-to-inelastic collisions. This condition was first demonstrated in 2D gases of fermionic KRb⁶¹, improving on the static shielding strategy in ref. 150. Cross-dimensional thermalization as a function of the

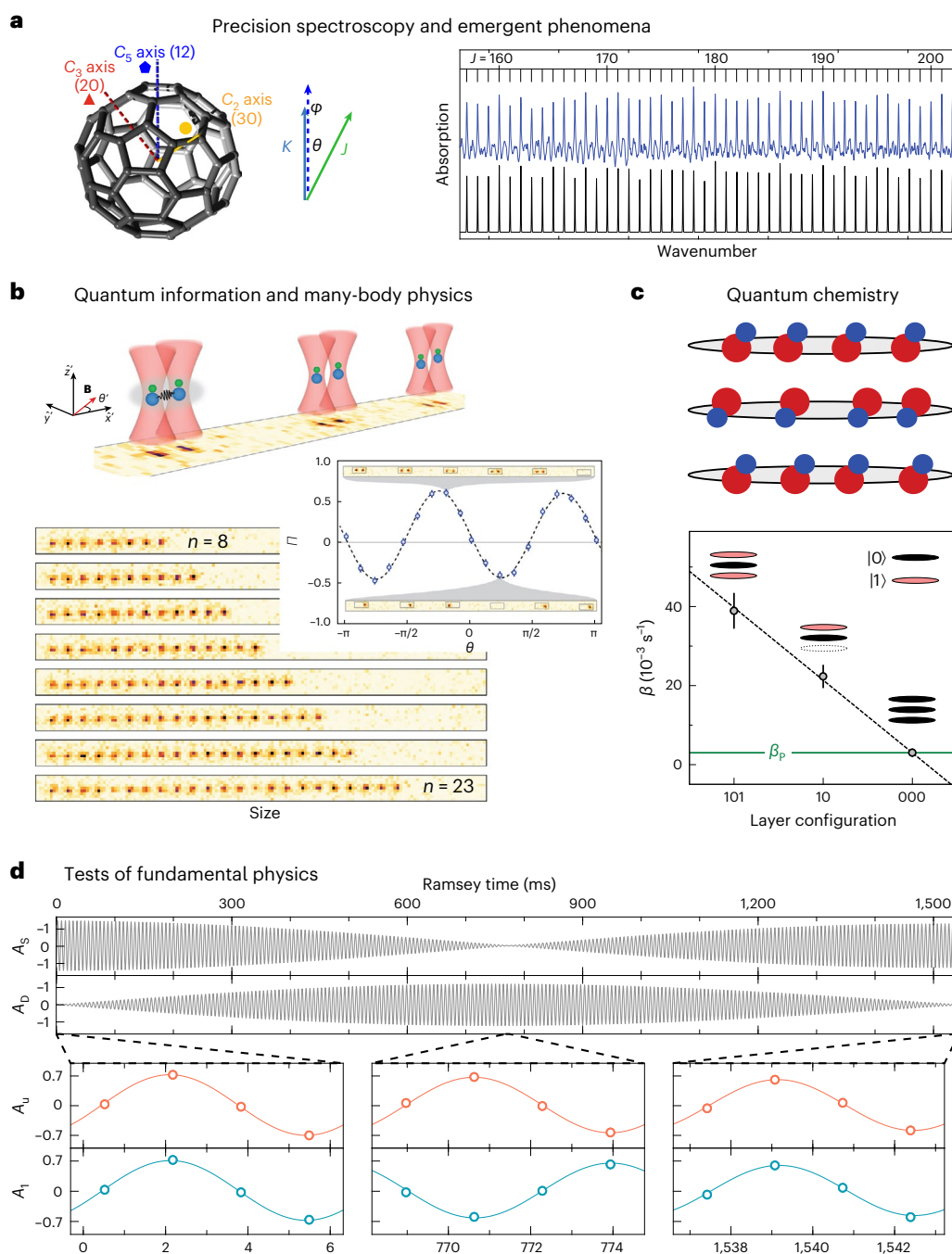


Fig. 5 | Advances in controlling intermediate-scale molecular systems.

a, Improved buffer gas cooling of large polyatomics, such as C_{60} , combined with advanced spectroscopy techniques, enables the probing of new features, such as ergodicity breaking in a mesoscopic quantum system. **b**, Tweezer arrays can be used to scale-up molecular systems from the single- to the many-molecule regime. Control over dipolar interactions in such arrays enables deterministic generation of an entangled Bell pair of individually trapped molecules. The inset shows coherent parity Π oscillations of the entangled Bell pairs^{26,27}. **c**, Tailored external fields can help engineer molecular structures with subwavelength

resolution. This facilitates the tuning of chemical reactivity by stacking spatially separated 2D layers of KRb molecules prepared in different rotational levels.

d, Ramsay interferometry with large, trapped samples of molecules showing coherence times exceeding a second, and providing the currently most stringent bound for the size of the electron's electric dipole moment. A_u and A_l are the fringe asymmetries for the upper and lower parity doublet, respectively. A_s and A_d represent the sum and difference asymmetries and are used to extract mean and difference frequencies, respectively. Panels adapted with permission from: **a**, refs. 10,11, AAAS; **b**, ref. 26, AAAS; **c**, ref. 74, AAAS; **d**, ref. 22, AAAS.

induced dipole moment revealed an optimum spot around 0.2D, where the separation among elastic and inelastic rate is maximum. This condition represented an ideal starting point for attempting evaporative cooling to quantum degeneracy, a necessary condition for any quantum simulation proposal. Controlled electric-field gradients enabled realization of the first degenerate Fermi gas from an initial thermal distribution of the molecules, relying on only the strength of molecular

interactions (Fig. 4e). The shielding resonance in ref. 157 was instead used to demonstrate evaporative cooling and phase-space-density increase in a 3D trap¹⁵⁸.

Evaporative cooling to quantum degeneracy was also demonstrated for a microwave-shielded gas of fermionic sodium–potassium (NaK) molecules⁶² (Fig. 4c). The large effective dipole moment enabled by microwave shielding allowed to approach the hydrodynamic regime

of collisions and an elastic-to-inelastic collisions ratio of 500. Recently, microwave shielding has led to the stabilization of quantum gases of bosonic alkali molecules, which could then be evaporatively cooled close to the onset of Bose degeneracy^{164,165}, and the formation of a molecular BEC⁶⁵.

The newly discovered Feshbach resonances provide an alternative path for molecule formation close to quantum degeneracy. In ref. 14, a new molecular quantum gas of weakly bound polyatomic molecules was demonstrated by adiabatic magneto-association of potassium atoms and sodium–potassium molecules in the rovibrational ground state, which may lead to the formation of ultracold ground-state polyatomics at record-high phase-space densities.

Scientific outlook

The use of cold molecules is now spreading across a variety of platforms for many different goals, including precision measurement, cold chemistry, quantum simulation and quantum information processing. Some of these topics are discussed in companion Reviews in this issue^{9,20,23,39}. It is clear that we are still at the very early stage of realizing the full potential of molecular quantum systems. Molecules are being employed in many-body physics experiments of increasing complexity (Fig. 5b), but many intriguing quantum phases remain unexplored or out of reach with the current capabilities. Quantum simulation employing precisely tunable interacting molecules offers fascinating opportunities to study exotic quantum phases and dynamics. Molecule-based precision measurements are setting new limits for violations of fundamental symmetries. When probed with state-of-the-art quantum control techniques, even molecular systems that have been known for decades reveal surprising, emergent phenomena (Fig. 5a). These achievements further support the dream of realizing fully quantum state-engineered molecules that are designed to have optimized sensitivity for fundamental physics. A first step in this direction is the trapping of large-scale samples of suitable molecules, including also polyatomics with favourable level structure for precision measurement applications (Fig. 5d). Incorporating modern spectroscopy and detection tools with cold molecules is allowing us to follow reaction pathways and kinetics, and steer these reaction processes with external fields and unprecedented spatial resolution (Fig. 5c). The exciting prospect of using quantum information science to explore complex molecular structure and uncover hidden interaction dynamics will breathe the powerful new life into quantum chemistry. Entanglement operations are being demonstrated on molecules trapped in optical fields, signalling initial steps in molecule-based quantum information processing (Fig. 5b), but the key challenges of achieving high fidelity and scalability are still open.

References

- Carr, L. D., DeMille, D., Kroms, R. V. & Ye, J. Cold and ultracold molecules: science, technology and applications. *New J. Phys.* **11**, 055049 (2009).
- Baranov, M. A., Dalmonte, M., Pupillo, G. & Zoller, P. Condensed matter theory of dipolar quantum gases. *Chem. Rev.* **112**, 5012–5061 (2008).
- Bohn, J. L., Rey, A. M. & Ye, J. Cold molecules: progress in quantum engineering of chemistry and quantum matter. *Science* **357**, 1002–1010 (2017).
- Di Rosa, M. D. Laser-cooling molecules. *Eur. Phys. J. D* **31**, 395–402 (2004).
- Stuhl, B. K., Sawyer, B. C., Wang, D. & Ye, J. Magneto-optical trap for polar molecules. *Phys. Rev. Lett.* **101**, 243002 (2008).
- Leung, K. H. et al. Terahertz vibrational molecular clock with systematic uncertainty at the 10^{-14} level. *Phys. Rev. X* **13**, 011047 (2023).
- Hu, M.-G. et al. Direct observation of bimolecular reactions of ultracold KRb molecules. *Science* **366**, 1111–1115 (2019).
- Bjork, B. J. et al. Direct frequency comb measurement of OD+CO→DOCO kinetics. *Science* **354**, 444–448 (2016).
- Karman, T., Tomza, M. & Perez-Rios, J. Ultracold chemistry as a testbed for few-body physics. *Nat. Phys.* [DOI TO COME] (2024).
- Changala, P. B., Weichman, M. L., Lee, K. F., Fermann, M. E. & Ye, J. Rovibrational quantum state resolution of the C₆₀ fullerene. *Science* **363**, 49–54 (2019).
- Liu, L. R. et al. Ergodicity breaking in rapidly rotating C₆₀ fullerenes. *Science* **381**, 778–783 (2023).
- Mitra, D. et al. Direct laser cooling of a symmetric top molecule. *Science* **369**, 1366–1369 (2020).
- Park, J. J., Lu, Y.-K., Jamison, A. O., Tscherbul, T. V. & Ketterle, W. A Feshbach resonance in collisions between triplet ground-state molecules. *Nature* **614**, 54–58 (2023).
- Yang, H. et al. Creation of an ultracold gas of triatomic molecules from an atom–diatomic molecule mixture. *Science* **378**, 1009–1013 (2022).
- Zhang, Z., Nagata, S., Yao, K.-X. & Chin, C. Many-body chemical reactions in a quantum degenerate gas. *Nat. Phys.* **19**, 1466–1470 (2023).
- Yan, B. et al. Observation of dipolar spin-exchange interactions with lattice-confined polar molecules. *Nature* **501**, 521–525 (2013).
- Hazzard, K. R. A. et al. Many-body dynamics of dipolar molecules in an optical lattice. *Phys. Rev. Lett.* **113**, 195302 (2014).
- Li, J.-R. et al. Tunable itinerant spin dynamics with polar molecules. *Nature* **614**, 70–74 (2023).
- Christakis, L. et al. Probing site-resolved correlations in a spin system of ultracold molecules. *Nature* **614**, 64–69 (2023).
- Cornish, S., Tarbutt, M. & Hazzard, K. Quantum computation and quantum simulation with ultracold molecules. *Nat. Phys.* [DOI TO COME] (2024).
- ACME Collaboration. Improved limit on the electric dipole moment of the electron. *Nature* **562**, 355–360 (2018).
- Roussy, T. S. et al. An improved bound on the electron's electric dipole moment. *Science* **381**, 46–50 (2023).
- DeMille, D., Hutzler, N., Rey, A.-M. & Zelevinsky, T. Quantum sensing and metrology with cold and ultracold molecules. *Nat. Phys.* [DOI TO COME] (2024).
- Ni, K.-K., Rosenband, T. & Grimes, D. D. Dipolar exchange quantum logic gate with polar molecules. *Chem. Sci.* **9**, 6830–6838 (2018).
- Hughes, M. et al. Robust entangling gate for polar molecules using magnetic and microwave fields. *Phys. Rev. A* **101**, 062308 (2020).
- Holland, C. M., Lu, Y. & Cheuk, L. W. On-demand entanglement of molecules in a reconfigurable optical tweezer array. *Science* **382**, 1143–1147 (2023).
- Bao, Y. et al. Dipolar spin-exchange and entanglement between molecules in an optical tweezer array. *Science* **382**, 1138–1143 (2023).
- Liang, Q. et al. Ultrasensitive multispecies spectroscopic breath analysis for real-time health monitoring and diagnostics. *Proc. Natl Acad. Sci. USA* **118**, 2105063118 (2021).
- Hutzler, N. R., Lu, H.-I. & Doyle, J. M. The buffer gas beam: an intense, cold, and slow source for atoms and molecules. *Chem. Rev.* **112**, 4803–4827 (2012).
- Segev, Y. et al. Molecular beam brightening by shock-wave suppression. *Sci. Adv.* **3**, 1602258 (2017).
- Wu, H. et al. Enhancing radical molecular beams by skimmer cooling. *Phys. Chem. Chem. Phys.* **20**, 11615–11621 (2018).
- van de Meerakker, S. Y. T., Bethlem, H. L., Vanhaecke, N. & Meijer, G. Manipulation and control of molecular beams. *Chem. Rev.* **112**, 4828–4878 (2012).
- Reens, D., Wu, H., Langen, T. & Ye, J. Controlling spin flips of molecules in an electromagnetic trap. *Phys. Rev. A* **96**, 63420 (2017).

34. Segev, Y. et al. Collisions between cold molecules in a superconducting magnetic trap. *Nature* **572**, 189–193 (2019).
35. Henson, A. B., Gersten, S., Shagam, Y., Narevicius, J. & Narevicius, E. Observation of resonances in Penning ionization reactions at sub-kelvin temperatures in merged beams. *Science* **338**, 234–238 (2012).
36. Vogels, S. N. et al. Imaging resonances in low-energy NO-He inelastic collisions. *Science* **350**, 787–790 (2015).
37. Wu, X. et al. A cryofuge for cold-collision experiments with slow polar molecules. *Science* **358**, 645–648 (2017).
38. Zeppenfeld, M. et al. Sisyphus cooling of electrically trapped polyatomic molecules. *Nature* **491**, 570–573 (2012).
39. Deiß, M., Willitsch, S. & Hecker-Denschlag, J. Cold trapped molecular ions and hybrid platforms for ions and neutral particles. *Nat. Phys.* [DOI TO COME] (2024).
40. Gadway, B. & Yan, B. Strongly interacting ultracold polar molecules. *J. Phys. B* **49**, 152002 (2016).
41. Moses, S. A., Covey, J. P., Miecnikowski, M. T., Jin, D. S. & Ye, J. New frontiers for quantum gases of polar molecules. *Nat. Phys.* **13**, 13–20 (2017).
42. Köhler, T., Góral, K. & Julienne, P. S. Production of cold molecules via magnetically tunable Feshbach resonances. *Rev. Mod. Phys.* **78**, 1311–1361 (2006).
43. Ni, K.-K. et al. A high phase-space-density gas of polar molecules. *Science* **322**, 231–235 (2008).
44. Danzl, J. G. et al. Quantum gas of deeply bound ground state molecules. *Science* **321**, 1062–1066 (2008).
45. Aikawa, K. et al. Coherent transfer of photoassociated molecules into the rovibrational ground state. *Phys. Rev. Lett.* **105**, 203001 (2010).
46. Takekoshi, T. et al. Ultracold dense samples of dipolar RbCs molecules in the rovibrational and hyperfine ground state. *Phys. Rev. Lett.* **113**, 205301 (2014).
47. Molony, P. K. et al. Creation of ultracold $^{87}\text{Rb}^{133}\text{Cs}$ molecules in the rovibrational ground state. *Phys. Rev. Lett.* **113**, 255301 (2014).
48. Park, J. W., Will, S. A. & Zwierlein, M. W. Ultracold dipolar gas of fermionic $^{23}\text{Na}^{40}\text{K}$ molecules in their absolute ground state. *Phys. Rev. Lett.* **114**, 205302 (2015).
49. Guo, M. et al. Creation of an ultracold gas of ground-state dipolar $^{23}\text{Na}^{87}\text{Rb}$ molecules. *Phys. Rev. Lett.* **116**, 205303 (2016).
50. Rvachov, T. M. et al. Long-lived ultracold molecules with electric and magnetic dipole moments. *Phys. Rev. Lett.* **119**, 143001 (2017).
51. Voges, K. K. et al. Ultracold gas of bosonic $^{23}\text{Na}^{39}\text{K}$ ground-state molecules. *Phys. Rev. Lett.* **125**, 083401 (2020).
52. Stevenson, I. et al. Ultracold gas of dipolar NaCs ground state molecules. *Phys. Rev. Lett.* **130**, 113002 (2023).
53. Cairncross, W. B. et al. Assembly of a Rovibrational Ground State Molecule in an Optical Tweezer. *Phys. Rev. Lett.* **126**, 123402 (2021).
54. Danzl, J. G. et al. An ultracold high-density sample of rovibronic ground-state molecules in an optical lattice. *Nat. Phys.* **6**, 265–270 (2010).
55. Barbé, V. et al. Observation of Feshbach resonances between alkali and closed-shell atoms. *Nat. Phys.* **14**, 881–884 (2018).
56. Deiglmayr, J. et al. Formation of ultracold polar molecules in the rovibrational ground state. *Phys. Rev. Lett.* **101**, 133004 (2008).
57. Lang, F., Winkler, K., Strauss, C., Grimm, R. & Denschlag, J. H. Ultracold triplet molecules in the rovibrational ground state. *Phys. Rev. Lett.* **101**, 133005 (2008).
58. Frye, M. D., Cornish, S. L. & Hutson, J. M. Prospects of forming high-spin polar molecules from ultracold atoms. *Phys. Rev. X* **10**, 041005 (2020).
59. Schäfer, F., Mizukami, N. & Takahashi, Y. Feshbach resonances of large-mass-imbalance Er–Li mixtures. *Phys. Rev. A* **105**, 012816 (2022).
60. Marco, L. D. et al. A degenerate Fermi gas of polar molecules. *Science* **363**, 853–856 (2019).
61. Valtolina, G. et al. Dipolar evaporation of reactive molecules to below the Fermi temperature. *Nature* **588**, 239–243 (2020).
62. Schindewolf, A. et al. Evaporation of microwave-shielded polar molecules to quantum degeneracy. *Nature* **607**, 677–681 (2022).
63. Duda, M. et al. Transition from a polaronic condensate to a degenerate Fermi gas of heteronuclear molecules. *Nat. Phys.* **19**, 720–725 (2023).
64. Cao, J. et al. Preparation of a quantum degenerate mixture of $^{23}\text{Na}^{40}\text{K}$ molecules and ^{40}K atoms. *Phys. Rev. A* **107**, 013307 (2023).
65. Bigagli, N. et al. Observation of Bose–Einstein condensation of dipolar molecules. Preprint at <https://arxiv.org/abs/2312.10965> (2023).
66. Liu, L. R. et al. Building one molecule from a reservoir of two atoms. *Science* **360**, 900–903 (2018).
67. Zhang, J. T. et al. Forming a single molecule by magneto-association in an optical tweezer. *Phys. Rev. Lett.* **124**, 253401 (2020).
68. Ruttley, D. K. et al. Formation of ultracold molecules by merging optical tweezers. *Phys. Rev. Lett.* **130**, 223401 (2023).
69. Ospelkaus, S. et al. Quantum-state controlled chemical reactions of ultracold potassium–rubidium molecules. *Science* **327**, 853–857 (2010).
70. Chotia, A. et al. Long-lived dipolar molecules and Feshbach molecules in a 3D optical lattice. *Phys. Rev. Lett.* **108**, 080405 (2012).
71. Park, J. W., Yan, Z. Z., Loh, H., Will, S. A. & Zwierlein, M. W. Second-scale nuclear spin coherence time of ultracold $^{23}\text{Na}^{40}\text{K}$ molecules. *Science* **357**, 372–375 (2017).
72. Kotochigova, S. & DeMille, D. Electric-field-dependent dynamic polarizability and state-insensitive conditions for optical trapping of diatomic polar molecules. *Phys. Rev. A* **82**, 063421 (2010).
73. Neyenhuis, B. et al. Anisotropic polarizability of ultracold polar $^{40}\text{K}^{87}\text{Rb}$ molecules. *Phys. Rev. Lett.* **109**, 230403 (2012).
74. Tobias, W. G. et al. Reactions between layer-resolved molecules mediated by dipolar spin exchange. *Science* **375**, 1299–1303 (2022).
75. Tarbutt, M. R. Laser cooling of molecules. *Contemp. Phys.* **59**, 356–376 (2018).
76. McCarron, D. Laser cooling and trapping molecules. *J. Phys. B* **51**, 212001 (2018).
77. Fitch, N. J. & Tarbutt, M. R. in *Advances in Atomic, Molecular, and Optical Physics* Vol. 70 (eds Dimauro, L. F. et al) 157–262 (Academic Press, 2021).
78. Barry, J. F., McCarron, D. J., Norrgard, E. B., Steinecker, M. H. & DeMille, D. Magneto-optical trapping of a diatomic molecule. *Nature* **512**, 286–289 (2014).
79. Truppe, S. et al. Molecules cooled below the Doppler limit. *Nat. Phys.* **13**, 1173–1176 (2017).
80. Anderegg, L. et al. Radio frequency magneto-optical trapping of CaF with high density. *Phys. Rev. Lett.* **119**, 103201 (2017).
81. Hummon, M. T. et al. 2D magneto-optical trapping of diatomic molecules. *Phys. Rev. Lett.* **110**, 143001 (2013).
82. Yeo, M. et al. Rotational state microwave mixing for laser cooling of complex diatomic molecules. *Phys. Rev. Lett.* **114**, 223003 (2015).
83. Ellis, A. M. Main group metal–ligand interactions in small molecules: new insights from laser spectroscopy. *Int. Rev. Phys. Chem.* **20**, 551–590 (2001).
84. Ding, S., Wu, Y., Finneran, I. A., Burau, J. J. & Ye, J. Sub-Doppler cooling and compressed trapping of YO molecules at μK temperatures. *Phys. Rev. X* **10**, 021049 (2020).
85. Collopy, A. L., Hummon, M. T., Yeo, M., Yan, B. & Ye, J. Prospects for a narrow line MOT in YO. *New J. Phys.* **17**, 55008 (2015).

86. Isaev, T. A. & Berger, R. Polyatomic candidates for cooling of molecules with lasers from simple theoretical concepts. *Phys. Rev. Lett.* **116**, 063006 (2016).
87. Augenbraun, B. L. et al. Direct laser cooling of polyatomic molecules. *Adv. At. Mol. Opt. Phys.* **72**, 89–182 (2023).
88. Kozyryev, I. et al. Sisyphus laser cooling of a polyatomic molecule. *Phys. Rev. Lett.* **118**, 173201 (2017).
89. Vilas, N. B. et al. Magneto-optical trapping and sub-Doppler cooling of a polyatomic molecule. *Nature* **606**, 70–74 (2022).
90. Ivanov, M. V., Bangerter, F. H., Wójcik, P. & Krylov, A. I. Toward ultracold organic chemistry: prospects of laser cooling large organic molecules. *J. Phys. Chem. Lett.* **11**, 6670–6676 (2020).
91. Zhu, G.-Z. et al. Functionalizing aromatic compounds with optical cycling centres. *Nat. Chem.* **14**, 995–999 (2022).
92. Kozyryev, I. & Hutzler, N. R. Precision measurement of time-reversal symmetry violation with laser-cooled polyatomic molecules. *Phys. Rev. Lett.* **119**, 133002 (2017).
93. Augenbraun, B. L., Doyle, J. M., Zelevinsky, T. & Kozyryev, I. Molecular asymmetry and optical cycling: laser cooling asymmetric top molecules. *Phys. Rev. X* **10**, 031022 (2020).
94. Maison, D. E., Flambaum, V. V., Hutzler, N. R. & Skripnikov, L. V. Electronic structure of the ytterbium monohydroxide molecule to search for axionlike particles. *Phys. Rev. A* **103**, 022813 (2021).
95. Kogel, F., Rockenhäuser, M., Albrecht, R. & Langen, T. A laser cooling scheme for precision measurements using fermionic barium monofluoride ($^{137}\text{Ba}^{19}\text{F}$) molecules. *New J. Phys.* **23**, 095003 (2021).
96. Zeng, Y. et al. Optical cycling in polyatomic molecules with complex hyperfine structure. *Phys. Rev. A* **108**, 012813 (2023).
97. Tarbutt, M. R. Magneto-optical trapping forces for atoms and molecules with complex level structures. *New J. Phys.* **17**, 015007 (2015).
98. Devlin, J. A. & Tarbutt, M. R. Three-dimensional Doppler, polarization-gradient, and magneto-optical forces for atoms and molecules with dark states. *New J. Phys.* **18**, 123017 (2016).
99. Cheuk, L. W. et al. Λ -enhanced imaging of molecules in an optical trap. *Phys. Rev. Lett.* **121**, 083201 (2018).
100. Shaw, J. C., Schnaubelt, J. C. & McCarron, D. J. Resonance Raman optical cycling for high-fidelity fluorescence detection of molecules. *Phys. Rev. Res.* **3**, 042041 (2021).
101. Rockenhäuser, M., Kogel, F., Pultinevicius, E. & Langen, T. Absorption spectroscopy for laser cooling and high-fidelity detection of barium monofluoride molecules. *Phys. Rev. A* **108**, 062812 (2023).
102. Truppe, S. et al. A buffer gas beam source for short, intense and slow molecular pulses. *J. Mod. Opt.* **65**, 648–656 (2018).
103. Barry, J. F., Shuman, E. S., Norrgard, E. B. & DeMille, D. Laser radiation pressure slowing of a molecular beam. *Phys. Rev. Lett.* **108**, 103002 (2012).
104. Truppe, S. et al. An intense, cold, velocity-controlled molecular beam by frequency-chirped laser slowing. *New J. Phys.* **19**, 022001 (2017).
105. Norrgard, E. B., McCarron, D. J., Steinecker, M. H., Tarbutt, M. R. & DeMille, D. Submillikelvin dipolar molecules in a radio-frequency magneto-optical trap. *Phys. Rev. Lett.* **116**, 063004 (2016).
106. Collopy, A. L. et al. 3D magneto-optical trap of yttrium monoxide. *Phys. Rev. Lett.* **121**, 213201 (2018).
107. McCarron, D. J., Steinecker, M. H., Zhu, Y. & DeMille, D. Magnetic trapping of an ultracold gas of polar molecules. *Phys. Rev. Lett.* **121**, 013202 (2018).
108. Anderegg, L. et al. Laser cooling of optically trapped molecules. *Nat. Phys.* **14**, 890–893 (2018).
109. Williams, H. J. et al. Magnetic trapping and coherent control of laser-cooled molecules. *Phys. Rev. Lett.* **120**, 163201 (2018).
110. Wu, Y., Burau, J. J., Mehling, K., Ye, J. & Ding, S. High phase-space density of laser-cooled molecules in an optical lattice. *Phys. Rev. Lett.* **127**, 263201 (2021).
111. Langin, T. K., Jorapur, V., Zhu, Y., Wang, Q. & DeMille, D. Polarization enhanced deep optical dipole trapping of Λ -cooled polar molecules. *Phys. Rev. Lett.* **127**, 163201 (2021).
112. Burau, J. J., Aggarwal, P., Mehling, K. & Ye, J. Blue-detuned magneto-optical trap of molecules. *Phys. Rev. Lett.* **130**, 193401 (2023).
113. Fitch, N. J. & Tarbutt, M. R. Principles and design of a Zeeman–Sisyphus decelerator for molecular beams. *ChemPhysChem* **17**, 3609–3623 (2016).
114. Petzold, M., Kaebert, P., Gersema, P., Siercke, M. & Ospelkaus, S. A Zeeman slower for diatomic molecules. *New J. Phys.* **20**, 042001 (2018).
115. Augenbraun, B. L. et al. Zeeman–Sisyphus deceleration of molecular beams. *Phys. Rev. Lett.* **127**, 263002 (2021).
116. Langin, T. K. & DeMille, D. Toward improved loading, cooling, and trapping of molecules in magneto-optical traps. *New J. Phys.* **25**, 043005 (2023).
117. Jadbabaie, A., Pilgram, N. H., Ktos, J., Kotochigova, S. & Hutzler, N. R. Enhanced molecular yield from a cryogenic buffer gas beam source via excited state chemistry. *New J. Phys.* **22**, 022002 (2020).
118. Son, H., Park, J. J., Ketterle, W. & Jamison, A. O. Collisional cooling of ultracold molecules. *Nature* **580**, 197–200 (2020).
119. Jurgilas, S. et al. Collisions between ultracold molecules and atoms in a magnetic trap. *Phys. Rev. Lett.* **126**, 153401 (2021).
120. Anderegg, L. et al. An optical tweezer array of ultracold molecules. *Science* **365**, 1156–1158 (2019).
121. Cheuk, L. W. et al. Observation of collisions between two ultracold ground-state CaF molecules. *Phys. Rev. Lett.* **125**, 43401 (2020).
122. Aldegunde, J., Rivington, B. A., Żuchowski, P. S. & Hutson, J. M. Hyperfine energy levels of alkali–metal dimers: ground-state polar molecules in electric and magnetic fields. *Phys. Rev. A* **78**, 033434 (2008).
123. Guo, M., Ye, X., He, J., Quéméner, G. & Wang, D. High-resolution internal state control of ultracold $^{23}\text{Na}^{87}\text{Rb}$ molecules. *Phys. Rev. A* **97**, 020501 (2018).
124. Ospelkaus, S. et al. Controlling the hyperfine state of rovibronic ground-state polar molecules. *Phys. Rev. Lett.* **104**, 030402 (2010).
125. Will, S. A., Park, J. W., Yan, Z. Z., Loh, H. & Zwierlein, M. W. Coherent microwave control of ultracold $^{23}\text{Na}^{40}\text{K}$ molecules. *Phys. Rev. Lett.* **116**, 225306 (2016).
126. Gregory, P. D., Aldegunde, J., Hutson, J. M. & Cornish, S. L. Controlling the rotational and hyperfine state of ultracold $^{87}\text{Rb}^{133}\text{Cs}$ molecules. *Phys. Rev. A* **94**, 041403 (2016).
127. Blackmore, J. A., Gregory, P. D., Bromley, S. L. & Cornish, S. L. Coherent manipulation of the internal state of ultracold $^{87}\text{Rb}^{133}\text{Cs}$ molecules with multiple microwave fields. *Phys. Chem. Chem. Phys.* **22**, 27529 (2020).
128. Ye, X., Guo, M., González-Martínez, M. L., Quéméner, G. & Wang, D. Collisions of ultracold $^{23}\text{Na}^{87}\text{Rb}$ molecules with controlled chemical reactivities. *Sci. Adv.* **4**, 0083 (2018).
129. Gorshkov, A. V. et al. Tunable superfluidity and quantum magnetism with ultracold polar molecules. *Phys. Rev. Lett.* **107**, 115301 (2011).
130. Wall, M., Hazzard, K. & Rey, A. M. in *From Atomic to Mesoscale: The Role of Quantum Coherence in Systems of Various Complexities* (eds Malinovskaya, S. A. & Novikova, I.) Ch. 1 (World Scientific, 2015).
131. Burchesky, S. et al. Rotational coherence times of polar molecules in optical tweezers. *Phys. Rev. Lett.* **127**, 123202 (2021).

132. Seeßelberg, F. et al. Extending rotational coherence of interacting polar molecules in a spin-decoupled magic trap. *Phys. Rev. Lett.* **121**, 253401 (2018).
133. Blackmore, J. A. et al. Controlling the ac Stark effect of RbCs with dc electric and magnetic fields. *Phys. Rev. A* **102**, 053316 (2020).
134. Bause, R. et al. Tune-out and magic wavelengths for ground-state $^{23}\text{Na}^{40}\text{K}$ molecules. *Phys. Rev. Lett.* **125**, 023201 (2020).
135. He, J. et al. Characterization of the lowest electronically excited-state ro-vibrational level of $^{23}\text{Na}^{87}\text{Rb}$. *New J. Phys.* **23**, 115003 (2021).
136. Gregory, P. D. et al. Second-scale rotational coherence and dipolar interactions in a gas of ultracold polar molecules. *Nat. Phys.* <https://doi.org/10.1038/s41567-023-02328-5> (2024).
137. Tscherbil, T. V., Ye, J. & Rey, A. M. Robust nuclear spin entanglement via dipolar interactions in polar molecules. *Phys. Rev. Lett.* **130**, 143002 (2023).
138. Gregory, P. D., Blackmore, J. A., Bromley, S. L., Hutson, J. M. & Cornish, S. L. Robust storage qubits in ultracold polar molecules. *Nat. Phys.* **17**, 1149–1153 (2021).
139. Lin, J., He, J., Jin, M., Chen, G. & Wang, D. Seconds-scale coherence on nuclear spin transitions of ultracold polar molecules in 3D optical lattices. *Phys. Rev. Lett.* **128**, 223201 (2022).
140. Böttcher, F. et al. New states of matter with fine-tuned interactions: quantum droplets and dipolar supersolids. *Rep. Prog. Phys.* **84**, 012403 (2020).
141. Chomaz, L. et al. Dipolar physics: a review of experiments with magnetic quantum gases. *Rep. Prog. Phys.* **86**, 026401 (2023).
142. Schmidt, M., Lassablière, L., Quéméner, G. & Langen, T. Self-bound dipolar droplets and supersolids in molecular Bose–Einstein condensates. *Phys. Rev. Res.* **4**, 013235 (2022).
143. Mayle, M., Quéméner, G., Ruzic, B. P. & Bohn, J. L. Scattering of ultracold molecules in the highly resonant regime. *Phys. Rev. A* **87**, 012709 (2013).
144. Christianen, A., Zwierlein, M. W., Groenenboom, G. C. & Karman, T. Photoinduced two-body loss of ultracold molecules. *Phys. Rev. Lett.* **123**, 123402 (2019).
145. Avdeenkov, A. V., Kajita, M. & Bohn, J. L. Suppression of inelastic collisions of polar $^1\Sigma$ state molecules in an electrostatic field. *Phys. Rev. A* **73**, 022707 (2006).
146. Gorshkov, A. V. et al. Suppression of inelastic collisions between polar molecules with a repulsive shield. *Phys. Rev. Lett.* **101**, 073201 (2008).
147. Karman, T. & Hutson, J. M. Microwave shielding of ultracold polar molecules. *Phys. Rev. Lett.* **121**, 163401 (2018).
148. Lassablière, L. & Quéméner, G. Controlling the scattering length of ultracold dipolar molecules. *Phys. Rev. Lett.* **121**, 163402 (2018).
149. Ni, K.-K. et al. Dipolar collisions of polar molecules in the quantum regime. *Nature* **464**, 1324–1328 (2010).
150. de Miranda, M. H. G. et al. Controlling the quantum stereodynamics of ultracold bimolecular reactions. *Nat. Phys.* **7**, 502–507 (2011).
151. Gregory, P. D. et al. Sticky collisions of ultracold RbCs molecules. *Nat. Commun.* **10**, 3104 (2019).
152. Guo, M. et al. Dipolar collisions of ultracold ground-state bosonic molecules. *Phys. Rev. X* **8**, 041044 (2018).
153. Gregory, P. D., Blackmore, J. A., Bromley, S. L. & Cornish, S. L. Loss of ultracold $^{87}\text{Rb}^{133}\text{Cs}$ molecules via optical excitation of long-lived two-body collision complexes. *Phys. Rev. Lett.* **124**, 163402 (2020).
154. Liu, Y. et al. Photo-excitation of long-lived transient intermediates in ultracold reactions. *Nat. Phys.* **16**, 1132–1136 (2020).
155. Bause, R. et al. Collisions of ultracold molecules in bright and dark optical dipole traps. *Phys. Rev. Res.* **3**, 033013 (2021).
156. Gersema, P. et al. Probing photoinduced two-body loss of ultracold nonreactive bosonic $^{23}\text{Na}^{87}\text{Rb}$ and $^{23}\text{Na}^{39}\text{K}$ molecules. *Phys. Rev. Lett.* **127**, 163401 (2021).
157. Matsuda, K. et al. Resonant collisional shielding of reactive molecules using electric fields. *Science* **370**, 1324–1327 (2020).
158. Li, J.-R. et al. Tuning of dipolar interactions and evaporative cooling in a three-dimensional molecular quantum gas. *Nat. Phys.* **17**, 1144–1148 (2021).
159. Anderegg, L. et al. Observation of microwave shielding of ultracold molecules. *Science* **373**, abg9502 (2021).
160. Chen, X.-Y. et al. Field-linked resonances of polar molecules. *Nature* **614**, 59–63 (2023).
161. Quéméner, G., Bohn, J. L. & Croft, J. F. E. Electroassociation of ultracold dipolar molecules into tetramer field-linked states. *Phys. Rev. Lett.* **131**, 043402 (2023).
162. Yang, H. et al. Observation of magnetically tunable Feshbach resonances in ultracold $^{23}\text{Na}^{40}\text{K} + ^{40}\text{K}$ collisions. *Science* **363**, 261–264 (2019).
163. Son, H. et al. Control of reactive collisions by quantum interference. *Science* **375**, 1006–1010 (2022).
164. Bigagli, N. et al. Collisionally stable gas of bosonic dipolar ground-state molecules. *Nat. Phys.* **19**, 1579–1584 (2023).
165. Lin, J. et al. Microwave shielding of bosonic NaRb molecules. *Phys. Rev. X* **13**, 031032 (2023).
166. Anderegg, L. *Ultracold Molecules in Optical Arrays: from Laser Cooling to Molecular Collisions*. PhD dissertation, Harvard Univ. (2019).

Acknowledgements

We thank P. Aggarwal, B. Augenbraun, L. Liu and A. M. Rey for comments and suggestions on the paper. T.L. acknowledges support from Carl Zeiss Foundation, the RiSC programme of the Ministry of Science, Research and Arts Baden-Württemberg, and the European Research Council (ERC) under the European Union’s Horizon 2020 research and innovation programme (grant agreement no. 949431). G.V. acknowledges support from the Alexander von Humboldt Foundation and the European Union (ERC, LIRICO 101115996). D.W. is supported by Hong Kong RGC General Research Fund (grants no. 14301818 and no. 14301119) and Collaborative Research Fund (grant no. C6009-20GF). J.Y. acknowledges support from ARO and AFOSR MRUI, and NIST.

Author contributions

All authors contributed to the writing of the paper.

Competing interests

The authors declare no competing interests.

Additional information

Correspondence and requests for materials should be addressed to Jun Ye.

Peer review information *Nature Physics* thanks the anonymous reviewers for their contribution to the peer review of this work.

Reprints and permissions information is available at www.nature.com/reprints.

Publisher’s note Springer Nature remains neutral with regard to jurisdictional claims in published maps and institutional affiliations.

This is a U.S. Government work and not under copyright protection in the US; foreign copyright protection may apply 2024